Physics of Fluids

Thermal effects on SARS-CoV-2 transmission in peristaltic blood flow: Mathematical modeling

Cite as: Phys. Fluids **34**, 061904 (2022); https://doi.org/10.1063/5.0095286
Submitted: 09 April 2022 • Accepted: 20 May 2022 • Accepted Manuscript Online: 21 May 2022 • Published Online: 13 June 2022

Dharmendra Tripathi, D. S. Bhandari and O. Anwar Bég

Physics of Fluids ARTICLE scitation.org/journal/phf

Thermal effects on SARS-CoV-2 transmission in peristaltic blood flow: Mathematical modeling

Cite as: Phys. Fluids **34**, 061904 (2022); doi: 10.1063/5.0095286
Submitted: 9 April 2022 · Accepted: 20 May 2022 ·
Published Online: 13 June 2022

Dharmendra Tripathi,[1,a)] D. S. Bhandari,[1] and O. Anwar Bég[2]

AFFILIATIONS

[1]Department of Mathematics, National Institute of Technology, Uttarakhand 246174, India
[2]Multi-Physical Engineering Sciences Group, Department Mechanical and Aeronautical Engineering, SEE, Salford University, Manchester, United Kingdom

Note: This paper is part of the special topic, Flow and the Virus.
[a)]**Author to whom correspondence should be addressed:** dtripathi@nituk.ac.in

ABSTRACT

SARS-CoV-2 is a novel viral species that has been identified as a highly infectious disease. Scientists have endeavored to collect essential information to better characterize the behavior of this virus, including droplet transmission and airborne effects. However, it is not clear, thus far, whether temperature can substantially alter the pandemic trajectory. This present study, therefore, aims to investigate how temperature may affect virus transmission in peristaltic blood vessels and, furthermore, how virus density and particle diameter will affect the transmission of the virus from an infected person to a non-infected person. The modeling deployed assumes that coronavirus particles with a diameter of 120 μm and a density of 1 g/cm^3 move in the direction of blood flow. The quantity of SARS-CoV-2 virions (entire virus particles) inside a microdroplet is calculated by considering the Kepler conjecture method, and the transmission percentage of the viral load is also computed. It is observed that the microdroplet carries a smaller amount of coronavirus particles, so an airborne ($D_P < 2\,\mu$m) infection is less harmful. Furthermore, computational simulations using the proposed model reveal some interesting insight into how rapidly the SARS-CoV-2 virus propagates in the circulatory system, and estimate the infection in blood and tissues. From these results, it is found that the small virion ($d_p < 100$ nm) rapidly settles inside the bloodstream and infects tissues; however, the duration of infection is short due to the low viscosity of the blood. Furthermore, the closed packed structure of the virions is loosened in the blood vessel due to the temperature of the blood.

NOMENCLATURE

c	Wave velocity (m/s)
d_p	Virion diameter (nm)
D_p	Droplet diameter (nm)
f_i	Hydrodynamic force (N)
g	Gravity (m/s^2)
L	Length of the blood vessel (m)
m	Mass of the fluid (kg)
m_p	Mass of the virion (kg)
N_p	Number of virions (–)
p	Blood flow at constant pressure (pa)
r	Radius of the virion (nm)
R_w	Width of the blood vessel (m)
t	Time scale (s)
T_0, T_1	Temperature at the center and wall, respectively (K)
u, v	Velocity components in the x–y direction, respectively (m/s)
U_i	Velocity of blood flow (m/s)
V_i	Velocity vector of the virion (m/s)
β	Heat source parameter (-)
ε	Wave number (-)
θ	Temperature (K)
κ	Thermal conductivity [W/(m K)]
λ	Wave length (-)
μ	Blood viscosity (Pa s)
ν	Kinematic viscosity (m^2/s)
ρ	Blood density (kg/m^3)
τ_p	Particle relaxation time (s)
τ_c	Fluid (blood) characteristic time (s)
ϕ	Amplitude of the wave propagation (m)
Φ	Specific heat source (W/m^2)
Φ	Stream function (-)

Dimensionless parameters

Gr	Grashof number (-)
Pr	Prandtl number (-)
Re	Reynolds number (-)
S	Density ratio (-)
S_N	Stokes number (-)
T_p	Transmission of virions (-)
V_T	Percentage of virion transmission (-)
β_1	Drag force parameter (-)
β_2	Virtual mass parameter (-)
β_3	Basset parameter (-)
β_4	Gravity parameter (-)

I. INTRODUCTION

In 2019, SARS-CoV-2 spread rapidly across the world and emerged as a global pandemic. It caused infection of the respiratory system in humans, which can vary from mild to lethal. With time, this virus has mutated into different strains and has taken many lives. Significant public safety measures were introduced to maintain control of the pandemic. In parallel, scientists attempted to assess and control key aspects of the virus including droplet transmission. The first species of this virus appeared in 1966, which was identified as two abnormal human respiratory viruses such as CoV-229E and CoV-B814.[1] These viruses were found in a spherical shape of size 80–120 nm in diameter through fluorescence and electron microscopy. Further studies showed that the droplet of virus particles does not settle with a size below 5 μm, which allows the virus particles to remain active in the air for a long time.[2] Some studies reported that the small sized droplet of the virion evaporates due to humidity and temperature effects.[3,4] In the context of SARS-CoV-2, researchers have discussed the outbreak of virus infection due to its seasonal nature.[3,5,6] However, a proper characterization of the impact of these parameters has remained elusive.

It is important to understand all the aspects that can control the spread of SARS-CoV-2. The behavior of virus particles inside the human body involves complex flow phenomena. The physical interpretation of virus transport inside blood vessels is essential for determining the transmission of coronavirus in the circulatory system. Furthermore, given the importance of flow phenomena in the transmission process, the methods, equipment, and practices employed to mitigate respiratory infections also involve fluid dynamics. In this regard, Maxey and Riley[7] have developed an expression for the motion of a particle inside a viscous fluid, using the Boussinesq–Basset equation as follows:

$$\frac{m_p d\bar{V}_i}{d\bar{t}} = (m_p - m)\bar{g} + m\frac{D\bar{U}_i}{D\bar{t}} + f_i. \tag{1}$$

Here, $\bar{V}_i = (u_p, v_p)$ is the velocity vector of the virus particle, $\bar{U}_i$ is the fluid velocity, and f_i is the hydrodynamic force exerted by the flow field. m_p is the particle mass, m is the mass of the fluid, and $\bar{g}$ is the gravity vector. The second term $(m\frac{D\bar{U}_i}{D\bar{t}})$ is a purely inertial contribution, which is the so-called added mass. It represents the additional mass the particle appears to possess due to the resistance to the acceleration of the surrounding fluid. The last term, f_i, is also known as disturbance force occurring in the fluid due to the particle and is expressed as follows:

$$f_i = -\frac{1}{2}m_i\{\bar{V}_i - \bar{U}_i\} - 6\pi r\mu\{\bar{V}_i - \bar{U}_i\} - 6\pi r^2\mu\left(\int_0^{\bar{t}} \frac{\left(\frac{d}{d\bar{t}}(\bar{V}_i - \bar{U}_i)\right)}{\sqrt{(\pi\nu(\bar{t}-\tau))}}d\tau + \frac{(V_{i_0} - \bar{U}_0)}{\sqrt{\bar{t}}}\right). \tag{2}$$

The equation of particle motion associated with the hydrodynamic force in viscous flow is the sum of steady-state drag force, the added mass force, and the Basset force. Generally, the Basset–Boussinesq expression describes the motion of a particle under transient hydrodynamic force exerted by Stokes drag and Basset force. Another concept of particle-fluid motion in two phases, i.e., fluid phase and particulate phase, was introduced in the literature to examine the particle motion based on the continuity and momentum equations without using the Boussinesq–Basset equation. The two phase particle-fluid motion based on mathematical models[8–10] has been reported and discussed the dusty fluid flow with various rheological properties. A virus laden particle motion over urinal flushing is simulated, and the mesh sensitivity analysis was performed.[11] They have reported that anti-diffusion improvements of facilities in public washrooms are required. Using the nano-particle transport equations, Islam *et al.*[12] analyzed how far SARS-CoV-2 particles can travel in the respiratory system and have reported that "the majority of SARS-CoV-2 aerosols are trapped at RL and RU lobes, and the minority is trapped at RM and LU lobes for 7.5 and 30 l/min airflow rates." Islam *et al.*[13] further demonstrated how coronavirus-2 aerosol propagates through age-specific upper airways. Finlay,[14] they presented the mechanics of the aerosol—in his book, Chap. III describes the motion of a single aerosol in a fluid medium. Holländer and Zaripov[15] investigated interactions of monodisperse 73 μm geometric diameter droplets with initial velocities between 1.5 and 3 m/s with the inclusion of the Basset force on the Maxey–Riley derivation.[7] Smith *et al.*[16] illustrate that highly infected people having a large viral load in their saliva and superspreaders producing lots of aerosols are likely to be far more dangerous transmitters of infection. Various studies[7–16] have reported on the movement of particles, aerosols, viruses, and droplets using diverse approaches, particularly with different formulations of the particle motion equation. However, no study has examined theoretically so far the virus movement in circulatory systems under the thermal effects and/or considered the simultaneous effects of blood viscosity, virus density, and diameter with peristaltic pumping.

To develop a novel mathematical model for the propagation of coronavirus through blood flow, we investigate theoretically the transient motion of particles in viscous flow with heat transfer through a peristaltic channel, a model of coronavirus transmission in peristaltic blood flow. Peristalsis is achieved via the rhythmic contraction and expansion of the walls of a distensible conduit, which generates efficient propulsion in blood flow and many other biological and bio-inspired applications.[17–22] In the present study, the kinematics of the channel wall induces the flow under peristaltic waves. The modeling deployed assumes that coronavirus particles with a diameter of 120 μm and a density of 1 g/cm^3 move in the direction of blood flow. The quantity of SARS-CoV-2 virions (entire virus particles) inside a microdroplet is calculated by considering the Kepler conjection

method, and the transmission percentage of viral load is also computed. Expressions are derived for the axial and transverse velocities of a coronavirus particle. Computations are performed to visualize the streamline profiles, the variation in the particle relaxation time with particle diameter, the distribution of number of virions (N_p) with SARS-CoV-2 diameter $d_p(\text{nm})$ for different particle diameters, and also the evolution of transmission virions (T_p) with SARS-CoV-2 diameter $d_p(\text{nm})$ for different virion transmission percentages (V_T). This study provides novel observations, which will aid in understanding how coronavirus transmits through blood flow in the circulatory system under the effects of thermal variation and rheological properties of different human blood characteristics. Here, we attempt to use well-established mathematical tools from fluid dynamics to understand why some individuals remain asymptomatic, whereas some die from COVID-19 infection. Furthermore, our analyses also partly explain the differential rate of clinical symptoms from the time since infection within severe cases.[23]

II. MATHEMATICAL MODEL

A. Governing equations

The modeling approach deployed herein adopts lubrication theory, i.e., blood flow occurs in a characteristic length of blood vessel much greater than the typical radius. Figure 1 depicts the virus transmission in blood flow through a vertical deformable vessel. Since a key objective of this study is to examine the influence of thermal effects on the transport of virus in peristaltic blood flow, heat transfer effects are included in the present model. The governing equations for the present biophysical model may be defined in the vectorial form as follows:

$$\nabla \cdot \bar{U}_i = 0, \tag{3a}$$

$$\rho\left(\left(\frac{\partial \bar{U}_i}{\partial \bar{t}}\right) + \bar{U}_i \cdot \nabla \bar{U}_i\right) = -\nabla \bar{p} + \mu\left(\nabla^2 \bar{U}_i\right) + \rho g \alpha (T - T_0), \tag{3b}$$

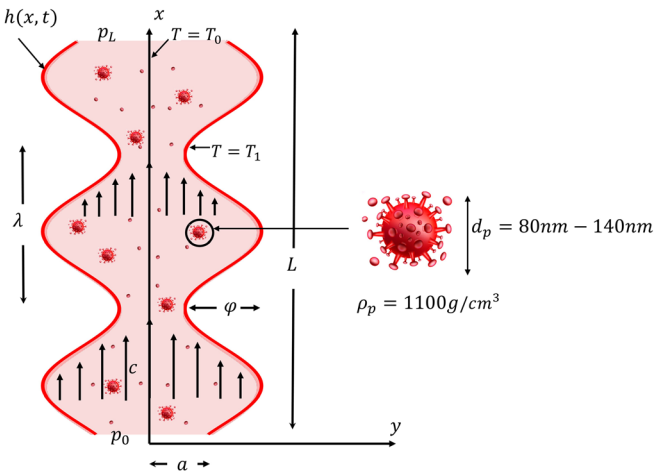

FIG. 1. Schematic representation of transmission of coronavirus particle through peristaltic blood flow.

$$\rho c_p\left(\frac{\partial \bar{T}}{\partial \bar{t}} + \nabla \cdot (\bar{V}_f\, \bar{T})\right) = \nabla \cdot (k \nabla \bar{T}) + \Phi, \tag{3c}$$

where $\bar{t}$ and $\bar{p}$ symbolize time and pressure, respectively. Blood is considered to be Newtonian with a density (ρ) of $1060\,\text{kg/m}^3$ (see Vijayaratnam *et al.*[24]).

B. Peristaltic wall motion

The nano-size coronavirus is propagating through peristaltic blood flow in circulatory system in the form of sinusoidal wave propagation. Mathematically, the peristaltic wall motion is expressed as

$$\bar{h}(\bar{x}, \bar{t}) = R_w - \bar{\phi}\cos^2\frac{\pi}{\bar{\lambda}}(\bar{x} - c\bar{t}), \tag{4}$$

where $\bar{h}$ is represented by a spatial-temporal wall function and $\bar{\phi}$ is the amplitude of the wave propagation. c and λ denote the arbitrary velocity and wavelength of the channel (blood vessel), respectively.

C. Dimensional scaling

It is pertinent to introduce scaling parameters $x = \frac{\pi\bar{x}}{\lambda}, y = \frac{\bar{y}}{R_w}$, $t = \frac{c\pi\bar{t}}{\lambda}$, $u = \frac{\bar{u}}{c}, v = \frac{\bar{v}}{c\varepsilon}, h = \frac{\bar{h}}{R_w}$, $\phi = \frac{\bar{\phi}}{R_w}$, and $p = \frac{\bar{p}\varepsilon R_w}{\mu c}$. Here, x, y, t, u, v, and p represent the dimensionless counterparts of the dimensional parameters. $R_w = a + \phi$ is the width of the channel, $\varepsilon = \pi\frac{R_w}{\lambda}$ is the wave number, $Re = \frac{\rho c R_w}{\mu}$ is a Reynolds number, $\nabla^2 = \varepsilon^2\frac{\partial^2}{\partial x^2} + \frac{\partial^2}{\partial y^2}$ is the Laplacian operator, $Gr = \frac{g\rho\alpha R_w^2(T_1 - T_0)}{\mu c}$ is the Grashof number, $\theta = \frac{T - T_0}{T_1 - T_0}$ is the temperature of the blood, $\beta = \frac{R_w^2\Phi}{k(T_1 - T_0)}$ is the heat source $(\beta > 0)$ or heat sink $(\beta < 0)$ parameter, and $Pr = \frac{\mu c_p}{k}$ is the Prandtl number. The conservation equations for the blood flow can, therefore, be reduced to

$$\left(\frac{\partial u}{\partial x} + \frac{\partial v}{\partial y}\right)\frac{\varepsilon c}{R_w} = 0, \tag{5a}$$

$$\varepsilon Re\left(\frac{\partial}{\partial t} + u\frac{\partial}{\partial x} + v\frac{\partial}{\partial y}\right)u = -\frac{\partial p}{\partial x} + \varepsilon^2\frac{\partial^2 u}{\partial x^2} + \frac{\partial^2 u}{\partial y^2} + Gr\theta, \tag{5b}$$

$$\varepsilon^2 Re\left(\frac{\partial}{\partial t} + u\frac{\partial}{\partial x} + v\frac{\partial}{\partial y}\right)v = -\frac{\partial p}{\partial y} + \varepsilon^3\frac{\partial^2 v}{\partial x^2} + \varepsilon\frac{\partial^2 v}{\partial y^2}, \tag{5c}$$

$$\varepsilon RePr\left(\frac{\partial \theta}{\partial t} + u\frac{\partial \theta}{\partial x} + v\frac{\partial \theta}{\partial y}\right) = \left(\varepsilon^2\frac{\partial \theta}{\partial x^2} + \frac{\partial^2 \theta}{\partial y^2}\right) + \beta. \tag{5d}$$

Under the lubrication approximation, low Reynolds number $(Re \in [0, \varepsilon])$, and large wavelength number $\varepsilon \ll 1$, where the viscous effect is dominant, neglecting the terms of $Re \in [0, \varepsilon]$, we obtain the following version of the conservation equations:

$$\frac{\partial u}{\partial x} + \frac{\partial v}{\partial y} = 0, \tag{6a}$$

$$\frac{\partial p}{\partial x} = \frac{\partial^2 u}{\partial y^2} + Gr\theta, \tag{6b}$$

$$\frac{\partial p}{\partial y} = 0, \tag{6c}$$

$$\frac{\partial^2 \theta}{\partial y^2} + \beta = 0. \tag{6d}$$

D. Boundary conditions

The boundary conditions are prescribed as follows:

$$At\ y=0,\quad \partial u/\partial y=0,\quad v=0,\quad \partial\theta/\partial y=0, \tag{7a}$$

$$At\ y=h,\quad u=0,\quad v=\frac{\partial h}{\partial t},\quad \theta=1, \tag{7b}$$

$$At\ x=0,\quad p=p_0(t), \tag{7c}$$

$$At\ x=1,\quad p=p_L(t). \tag{7d}$$

E. Analytical solutions

The blood temperature is derived as follows:

$$\theta=\frac{1}{2}(2+\beta(h^2-y^2)). \tag{8}$$

Axial blood velocity is obtained as

$$u=\frac{1}{2}\frac{\partial p}{\partial x}\left(y^2-h^2\right)-\frac{1}{24}Gr(12+\beta(5h^2-y^2))(y^2-h^2). \tag{9}$$

By considering the continuity equation (6a), the transverse blood velocity emerges as

$$v=\frac{1}{6}\left(3h^2y-y^3\right)\frac{\partial^2 p}{\partial x^2}+yh\frac{\partial p}{\partial x}\frac{\partial h}{\partial x}+\frac{1}{6}yhGr(-6+y^2\beta-5\beta h^2)\frac{\partial h}{\partial x}. \tag{10}$$

As $v|_{y=h}=\partial h/\partial t$, the wall deformation rate is obtained as

$$\frac{\partial h}{\partial t}=\frac{1}{3}\frac{\partial^2 p}{\partial x^2}h^3+\frac{\partial p}{\partial x}\frac{\partial h}{\partial x}h^2-\frac{\partial h}{\partial x}h^2Gr-\frac{2}{3}\frac{\partial h}{\partial x}\beta Grh^4. \tag{11}$$

Integrating Eq. (11) with respect to x, the pressure gradient is derived as

$$\frac{\partial p}{\partial x}=3\frac{1}{h^3}\int_0^x\frac{\partial h}{\partial t}dx+\frac{2}{5}\beta Grh^2+\frac{3}{h^3}G_0(t)+Gr. \tag{12}$$

Here, $G_0(t)$ is a pressure gradient parameter, defined as

$$G_0(t)=\frac{\frac{1}{3}\left(\Delta p-3\int_0^1\left(\frac{1}{h^3}\int_0^x\frac{\partial h}{\partial t}dx\right)dx-\frac{2}{5}\beta Gr\int_0^1h^2dx-Gr\right)}{\int_0^1\frac{1}{h^3}dx}. \tag{13}$$

The stream function that defines the relation between the flow field and the velocity profile takes the following form:

$$\psi=\frac{1}{120}(y-h)^2\left(20\frac{\partial p}{\partial x}(y+2h)+Gr\left(y(-20+y^2\beta)-h\left(40-2y^2\beta+\beta h(7y+16h)\right)\right)\right). \tag{14}$$

III. RESULTS AND DISCUSSION

A. Blood velocity profiles and streamlines

In this section, the velocity vectors and flow field behavior corresponding to peristaltic blood flow in the channel (blood vessel) are addressed. The particles are allowed to propagate in the fluid under the influence of Stokes force and the constant gravitational field. Typically, the diameter of the blood vessel is within the range 1–20 μm as referred in Tu *et al.*[25] The velocity of the fluid particle in the blood vessel varies from approximately 1 mm/s to 50 cm/s.[26,27] Figure 2 represents the velocity vector pattern inside the channel with $\phi=0.4$ and $t=0.1$. In the numerical computations, two cases are analyzed: (a) $Gr=0$, $\beta=0$, without thermal effects and (b) $Gr=1$, $\beta=2$, with thermal effects. Here, a stagnation line is present at the center, which bifurcates the velocity vector at the relaxation region. On the contrary, the propagative flow field acts at the contraction region, which propels the physiological fluid in the upward (forward) direction. This mechanism controls the blood flow in the vessel. In addition, the impact of buoyancy force [i.e., the Grashof number (Gr)] and heat source ($\beta>0$) on streamlines of the velocity vector is illustrated through Figs. 2(a) and 2(b), respectively. From these figures, it is observed that both parameters are responsible for the smooth and high velocity in the blood vessel (i.e., when the body temperature rises, blood flow inside the

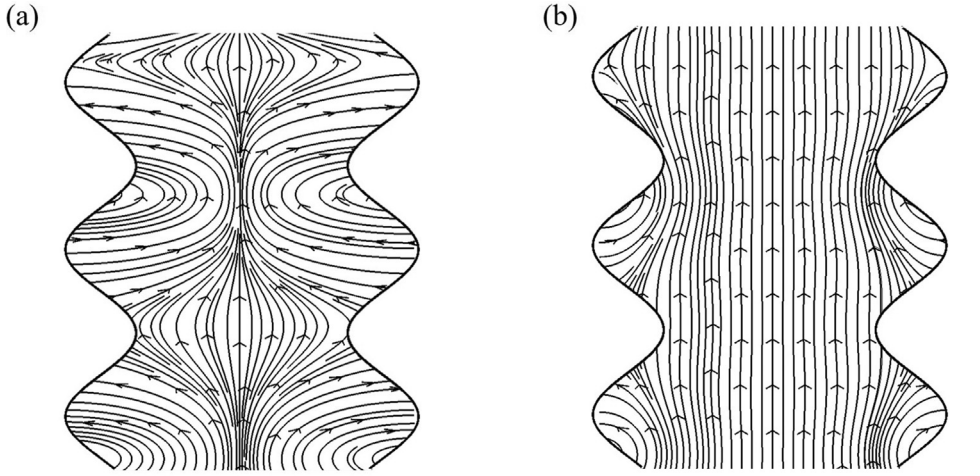

FIG. 2. Streamlines of the blood velocity vectors for (a) $Gr=0$, $\beta=0$ and (b) $Gr=1$, $\beta=2$.

circulatory system increases). Figures 3(a) and 3(b) show the stream function contours of the u–v vector, and excess of a fivefold boost in magnitudes is observed from the non-thermal case (a) $Gr = 0$ and $\beta = 0$ to the thermal case (b) $Gr = 1$ and $\beta = 2$. In particular, there is a strong alignment in streamlines along the central (core) channel zone, indicating that the flow is intensified in the vessel with heat source and thermal buoyancy forces. Effectively, therefore, the presence of heat transfer (natural convection) and heat generation, which characterizes real blood flows, encourages acceleration in the vessel.

B. Virus transport in peristaltic blood flow

The transport of a small size virion in the blood vessel can be described by the Boussinesq–Basset equation. This equation expresses the transient hydrodynamic force that helps to correlate the motion of the nano-size particles subject to uniform/non-uniform flow in the circulatory system, and it is mathematically expressed as

$$\frac{m_p d\bar{V}_i}{d\bar{t}} = (m_p - m)\bar{g} + m_f \frac{D\bar{U}_i}{D\bar{t}} - \frac{1}{2} m \bar{V}_i - \bar{U}_i - 6\pi r \mu \bar{V}_i - \bar{U}_i - 6\pi r^2 \mu \left(\int_0^{\bar{t}} \frac{\left(\frac{d}{d\bar{t}} (\bar{V}_i - \bar{U}_i) \right)}{\sqrt{(\pi \nu (\bar{t} - \tau))}} d\tau + \frac{(V_{i_0} - U_{i_0})}{\sqrt{\bar{t}}} \right). \quad (15)$$

Here, $r = \frac{d_p}{2}$ is the particle radius (d_p is the particle diameter). Jiménez-Lozano *et al.*[27] have shown that the influence of drag force contributes more significantly the particles motion in fluid medium, for example, micro-size bacteria particles in the ureter, rather than all the other forces acting on the particle motion. Kim *et al.*[28] have noted that if the density of the particle is lower than fluid density, then several fluid forces such as buoyancy force, Basset force, pressure force, and Faxen corrections (wherein the Stokes drag force acting on a particle is increased due to the presence of a neighboring wall) may affect the particle motion. The following dimensionless quantities are implemented in Eq. (15) to utilize suitable assumptions:

$$u_p = \frac{\bar{u}_p}{c}, \quad v_p = \frac{\bar{v}_p}{c}, \quad g = \frac{\bar{g}}{g_0}, \quad \tau_c = \frac{\lambda}{\pi c}, \quad \tau_p = \frac{\rho_p d_p^2}{18\mu}, \quad \alpha = \frac{d_p}{R_w}, \quad S_N = \frac{\tau_p}{\tau_c}, \quad S = \rho_p/\rho_f. \quad (16)$$

Here, the convective acceleration (Stokes flow) approximating the substantial derivative $\left(\frac{D}{Dt}\right)$ as $\left(\frac{d}{dt}\right)$ is exact to the order of approximation required for uniform blood flows. The Boussinesq–Basset equation can now be written as

$$\frac{dV_i}{dt} = \frac{1}{S_N}\left(\frac{2S}{2S+1}\right)(V_i - U_i) + \frac{3}{2S+1}\frac{dU_i}{dt} + \sqrt{\frac{9}{2\pi S S_N}}\left(\frac{2S}{2S+1}\right)\left(\int_0^{\bar{t}} \frac{\left(\frac{d}{d\bar{t}} (V_i - U_i) \right)}{\sqrt{t - \tau}} d\tau + \frac{(V_{i0} - U_{i0})}{\sqrt{t}} \right) + \frac{2(S-1)}{2S+1}\frac{\tau_c}{c} g_0 g. \quad (17)$$

The axial and transverse components of the virion velocity vector are expressed as

$$\frac{du_p}{dt} = \beta_1 (u - u_p) + \beta_2 \frac{du}{dt} + \beta_3 \left(\int_0^t \frac{\left(\frac{d}{dt} (u - u_p) \right)}{\sqrt{t - \tau}} d\tau + \frac{(u_0 - u_{p0})}{\sqrt{t}} \right), \quad (18)$$

$$\frac{dv_p}{dt} = \beta_1 (v - v_p) + \beta_2 \frac{dv}{dt} + \beta_3 \left(\int_0^t \frac{\left(\frac{d}{dt} (v - v_p) \right)}{\sqrt{t - \tau}} d\tau + \frac{(v_0 - v_{p0})}{\sqrt{t}} \right) - \beta_4. \quad (19)$$

Here

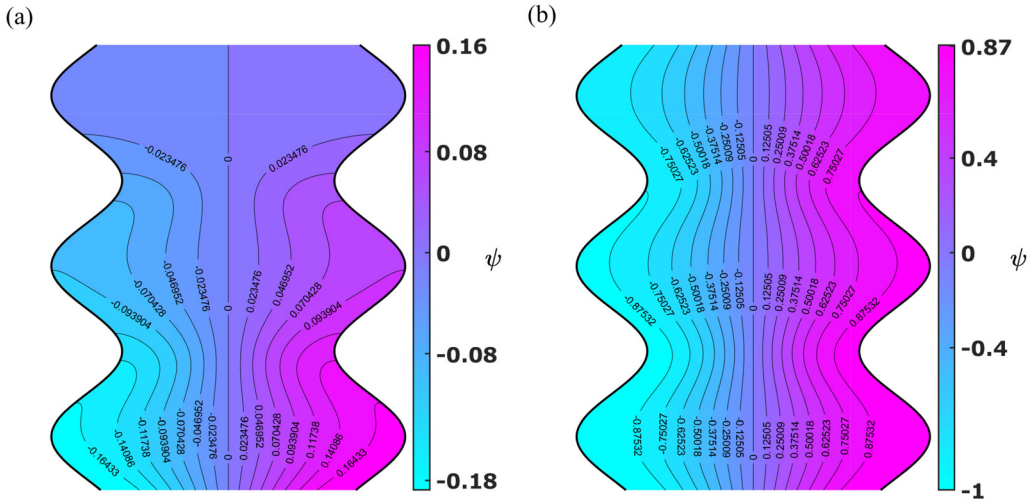

FIG. 3. Contour of the stream function for (a) $Gr = 0$, $\beta = 0$ and (b) $Gr = 1$, $\beta = 2$.

TABLE I. Parametric values of circulatory system (blood stream).

Parameters definition	Length of the blood vessel (L; mm)	Wave velocity (c; mm/s)	Blood density (ρ; kg/m^3)	Gravity (g_0; m/s^2)	Fluid (blood) characteristic time ($\tau_c = \frac{L}{\pi c}$)
Point Estm.	120	300–400	1060	1	0.127

$$\beta_1 = \frac{1}{S_N}\left(\frac{2S}{2S+1}\right), \quad \beta_2 = \frac{3}{2S+1}, \quad \beta_3 = \sqrt{\frac{9}{2\pi S S_N}}\left(\frac{2S}{2S+1}\right), \quad \beta_4 = \frac{2(S-1)}{2S+1}\frac{\tau_c}{c}g_0 g. \tag{20}$$

In the present theoretical study of virus transmission in peristaltic blood flow, it is of interest to analyze also the effect of fluid temperature on the transmission of virus. In this respect, axial and transverse velocity components of the virus particle are derived as the solutions of Eqs. (18) and (19) subject to boundary condition $u_p|_{t=0} = 0$, and $v_p|_{t=0} = 0$, as follows:

$$u_p = I_0 \int_0^t I_1 \left(\beta_1 u + \beta_2 \frac{du}{dt} + 1.41\beta_3 \frac{u}{\sqrt{t}}\right) dt, \tag{21}$$

$$v_p = I_0 \int_0^t I_1 \left(\beta_1 v + \beta_2 \frac{dv}{dt} + 1.41\beta_3 \frac{v}{\sqrt{t}} - \beta_4\right) dt, \tag{22}$$

where $I_0 = e^{-\beta_1 t} e^{-2.82\beta_5\sqrt{t}}$ and $I_1 = e^{\beta_1 t} e^{2.82\beta_5\sqrt{t}}$.

C. Parameter selection

Based on the data available in the literature,[26] the appropriate clinical parametric details were selected for the virus and blood and further computed other parameters' values/ranges for the simulation of virus movement through peristaltic blood flow and tabulated in Tables I and II, respectively.

From Table II, the average value of $\boldsymbol{\beta_1}$: 3.56×10^8 and $\boldsymbol{\beta_3} = 1.822 \times 10^4$ is considered for the computation of the results.

D. Transmission of SARS-CoV-2 by droplet particle packing

This has been a matter of discussion whether the virus can transmit by air or not. Some studies report that virus spread is reduced as the size of the microdroplet particle is increased, see Refs. 16 and 29. Thomas[30] has reported that the range of the microdroplet particle is 1 μm (even smaller) to 2 mm. Many studies reported that the microdroplet particle $<5\,\mu$m constitutes an aerosol. On the contrary, Mathews *et al.*[31] have demonstrated that the microdroplet particle contains the minimum amount of gel form as compared to the contribution of virion, which make them solid aerosols. In this regard, Nor *et al.*[32] have noted that a virus can be transported via solid aerosols. Furthermore, it is important to know how many virions of SARS-CoV-2 transmit from an infected person to non-infected person, which helps to protect the vulnerable and control the spread of the SARS-CoV-2 infection. Figure 4 shows the mechanism of transmission of virion infection from an infected person to a non-infected person. During the interaction, the virion droplet that resides in the infected person (red head) is transferred to another person (green head) via human activity, including coughing, talking, laughing, sneezing, etc.

In this study, the Kepler conjecture is deployed, which provides a theorem for the optimal packaging of virions in a droplet particle. Following Hales,[33] the Kepler approach considers that the density of compact packing arrangements is around $\pi/\sqrt{18} = 74.048$. Since coronavirus particles are assumed to possess a spherical shape, the possible amount of virions of diameter $d_p = 80$–140 nm that can be packaged in a droplet diameter $D_p = 2$–$100\,\mu$m (consider) is defined as follows:

$$N_p = 74.048 \frac{\text{volume of the droplet}}{\text{volume of the particle}}. \tag{23}$$

Thus far, the distinction between the size of microdroplet particles (i.e., either aerosol or droplet) has been discussed. A key question is whether aerosol particles are responsible for the infection transmission from person to person? As noted by Thomas,[30] the majority of SARS-CoV-2 virions that reside in the respiratory tract of an infected person (i.e., less than 10 μm the droplet) are 78%–96% in the form of microdroplets, while only 4%–46% of virus particles are produced during coughing and sneezing. From

TABLE II. Estimates of parameters associated with novel coronavirus SARS-CoV-2 at the average density ρ_p of virus in the blood stream 1100 kg/m^3.

Parameter definition	Formula	Parametric range of blood viscosity and virus diameter Blood viscosity ($\boldsymbol{\mu}$): 3.3×10^{-3} Ns/m^2 Virus diameter ($\boldsymbol{d_p}$): 80–140 nm
The particle relaxation time ($\boldsymbol{\tau_p}$)	$\frac{\rho_p d_p^2}{18\mu}$	$(1.185 - 3.629) \times 10^{-10}$
Stokes number ($\boldsymbol{S_N}$)	τ_p/τ_c	$(0.933$–$2.857) \times 10^{-9}$
Density ratio ($\boldsymbol{S}$)	ρ_p/ρ	1.037
Drag force ($\boldsymbol{\beta_1}$)	$\frac{1}{S_N}\left(\frac{2S}{2S+1}\right)$	$(7.231$–$2.361) \times 10^8$
Virtual mass force ($\boldsymbol{\beta_2}$)	$\frac{3}{2S+1}$	0.976
Basset ($\boldsymbol{\beta_3}$)	$\sqrt{\frac{9}{2\pi S S_N}}\left(\frac{2S}{2S+1}\right)$	$(2.596$–$1.483) \times 10^4$
Gravity ($\boldsymbol{\beta_4}$)	$\frac{2(S-1)}{2S+1}\frac{\tau_c}{c}g_0 g$	0.099

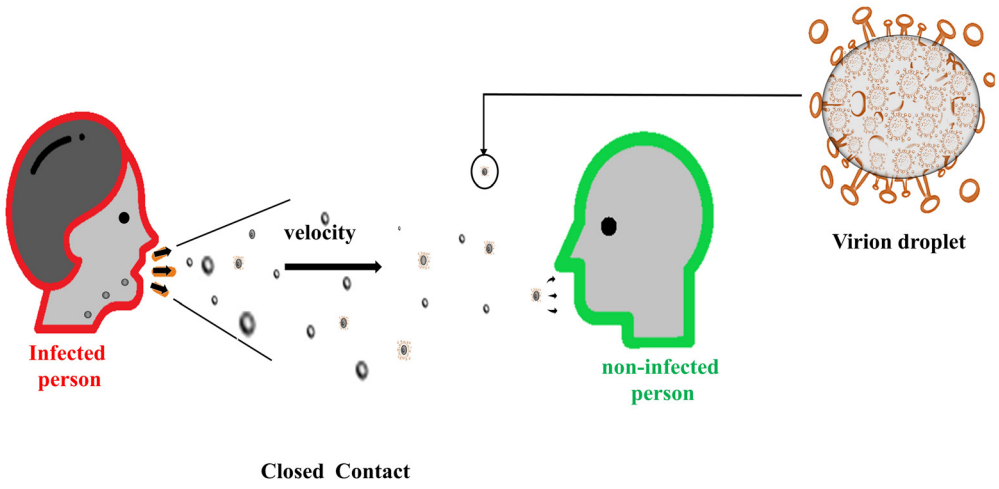

FIG. 4. An illustration of transmission of virion infection from an infected person to a non-infected person.

Fig. 5, it is observed that the nano-size SARS-CoV-2 virus particle can reside inside the microdroplet of an infected person. Here, the number of SARS-CoV-2 virions is 10^6 in the droplet of 2 μm, while 10^7 virions are reported for the droplet of 10 μm. This result shows that as the microdroplet size is decreased, they carry less quantities of coronavirus particles that is why an airborne infection is less harmful, which has also been documented by Smith[16] and Bhat *et al.*[34] The transmission of SARS-CoV-2 virus particles from one infected person to non-infected person is illustrated in Fig. 6. The transmission of virus particles depends on the oral and nasal activity of the human (such as breathing, talking, laughing, coughing, and sneezing). In the context of human activity, we have considered three possibilities of virion transmission (such as 10%, 20%, and 30%) during the coughing and sneezing in the droplet of diameter 5 μm. The magnitude of the number of SARS-CoV-2 virions is 10^6 in the aerosol particle (5 μm). If the percentage of transmission of the aerosol particle is less with a low viral load (the amount of virion makes a person sick), there is not much impact of infection to another person. However, if the viral load is high or the transmission percentage is large, the non-infected person may be infected.

E. Estimate of infection transmission through blood flow

It has been noticed that the transmission of infection from person to person through coughing, talking, laughing, and sneezing mainly depends on the density and initial velocity of the virion droplet from the nasal zone or mouth. Initially, some smaller size virions are rapidly evaporated due to the humidity and temperature of the local environment, as elaborated earlier by Gralton *et al.*[35] and Fernstrom and Goldblatt.[36] The remaining virions either travel in the air or fall to the ground depending on the size and density of the microdroplet. During the process of inhalation, some aerosol particles avoid getting trapped in the mucus and cilia, and they are deposited in the bronchoalveolar region of the lungs, liver, heart, and stomach. The virions entering the body mainly depend on the droplet characteristic such as droplet size, droplet velocity, temperature, type of pathogen, the activity of pathogen, etc. Among these parameters, we have considered the blood vessel as a pathway via peristaltic motion that transports the blood containing virus in the circulatory system. Once the SARS-CoV-2 virus (droplets) has entered the circulatory system through the nose or mouth, some time is required before they settle within the bloodstream.

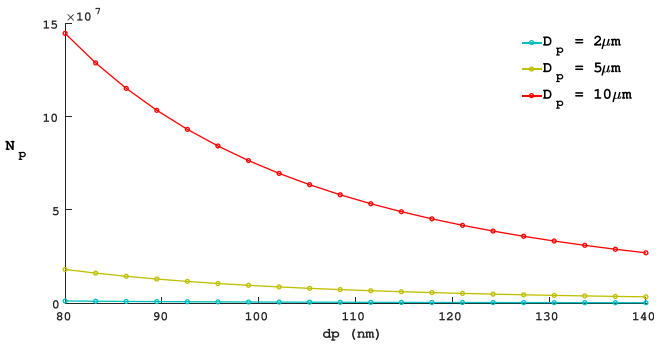

FIG. 5. Number of virions (N_p) with SARS-CoV-2 diameter d_p(nm) for different droplet diameters.

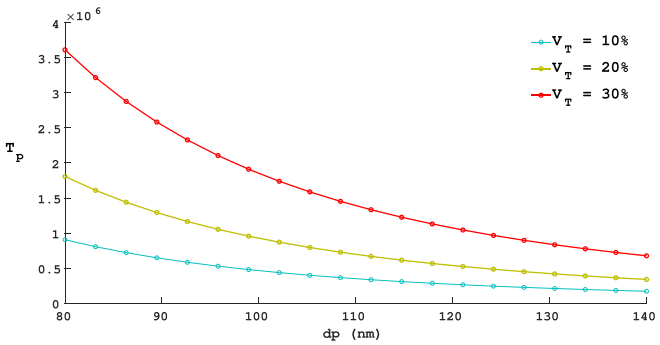

FIG. 6. Number of transmission virions (T_p) with SARS-CoV-2 diameter d_p(nm) for different virion transmission percentages (V_T).

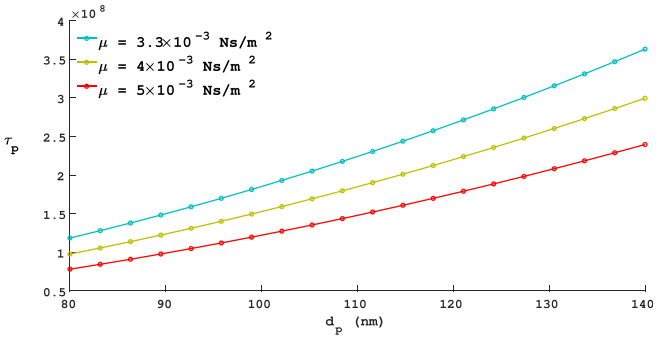

FIG. 7. The variation in the particle relaxation time with particle diameter at a fixed value of $\phi = 0.4$ and $x = 0.3$.

Figure 7. The variation of the virion particle relaxation time with SARS-CoV-2 virion diameter for different blood viscosities. This figure shows that the small size virus particle ($d_p = 80$ nm) rapidly settles inside the bloodstream as compared to large size virus particles ($d_p = 140$ nm). Furthermore, it is observed that the virions take more time to settle in blood with lower viscosity. This would indicate that the infection period time is less for lower viscosity blood.

F. Thermal effects on the transmission of SARS-CoV-2 through blood flow

Using the mathematical model described earlier, it is possible to analyze the progression of SARS-CoV-2 through a blood vessel. Additionally, the effect of temperature and applicable forces on the transmission of SARS-CoV-2 has been computed. In this mathematical model, parameters such as diameter and density of the virus particle, and viscosity of the blood have been considered to achieve more accurate results as presented in Table I. From the literature, it is observed that the peristaltic pumping mechanism transports the nano-size particle/molecules along the direction of blood flow within the velocity range of 300–400 mm/s in humans.

Figure 8 illustrates that how the SARS-CoV-2 virus particle moves through the blood vessel. Since the axial velocity of the fluid is zero at the wall of the blood vessel (due to the consideration of no-slip boundary condition), the particle axial velocity is also zero, which validates our result. The wave-like progression of the virion velocity is influenced naturally via the peristaltic (contraction and relaxation of the blood vessel) movement of the blood in the circulatory system. The axial virion attains high velocity (of the order of multiples of 10^7) in the blood vessel. In other words, once the virus particle enters the physiological systems, it will rapidly move along with the bloodstream and spread throughout the cardiovascular system. Typically, body temperature exerts a key role in influencing blood flow in the circulatory system. Further blood absorbs and distributes heat throughout the physiological system. When bacteria/viruses enter inside the body, the blood vessels react rapidly via expansion and contraction of the blood vessel. The actuation of the blood vessel transports the blood and heat (thermal energy) to other locations, whenever it is required. Consequently, the axial velocity of the particle is slightly increased with heat generation (source) ($\beta = 5$), as shown in Fig. 8. From the physical point of view, the closed packed structure of the virions is lossened in the blood vessel due to the more temperature of the blood. Therefore, the arrangement of packing densities will decrease, and they will be separated from each other, resulting in a reduction in the innervation of tissues and blood vessels. Furthermore, the viscosity of the blood becomes reduced as $\mu = (2(\rho_p - \rho) * g * a^2)/(9 * v)$, and hence, blood circulation is improved, which further amplifies virion transport in the system.

Figure 9 illustrates the impact of thermal buoyancy force on the motion of the virion. The Grashof number (Gr) is the ratio of the buoyancy force to viscous force. Earlier, we discussed that if the particle density is less than the fluid density, the dynamics of particle flow becomes complex. The buoyancy force is one of the fluid forces that can affect the motion of the virus when the fluid density is greater than the particle density. From Fig. 9, it is observed that the Gr is responsible for the large axial velocity of the virion, i.e., the SARS-CoV-2 particle is strongly influenced via the upthrust associated with free convection currents. It will remain suspended continuously and take time to settle at the surface body/tissues, so that it will take time to damage the tissues (internal organs). The case $Gr = 0$ corresponds to forced convection, for which thermal buoyancy is absent. Furthermore, the transient behavior of axial velocity of the virus particle at a fixed position $x = 0.3$ is displayed in Fig. 10 with the effect of heat generation (β). The profiles computed show that the particle behavior is almost uniform throughout time. With increasing heat source parameter, the thermal effect is increased, and the axial particle velocity is slightly increased, but only after a critical time elapse. In

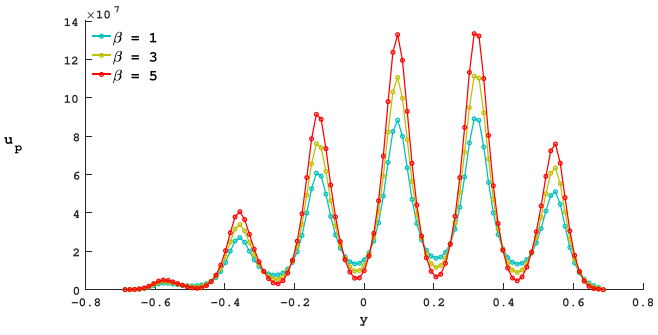

FIG. 8. The variation in the axial virus velocity for different values of heat source parameter (β) at a fixed value of $\phi = 0.4$, $t = 0.4$, and $x = 0.2$.

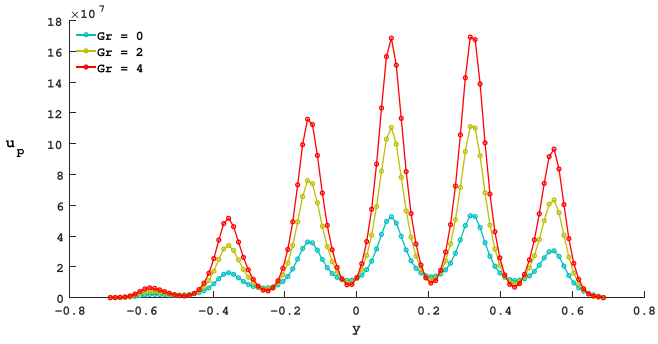

FIG. 9. The variation in the axial virus velocity for different values of the Grashof number at a fixed value of $\phi = 0.4$, $t = 0.4$, and $x = 0.2$.

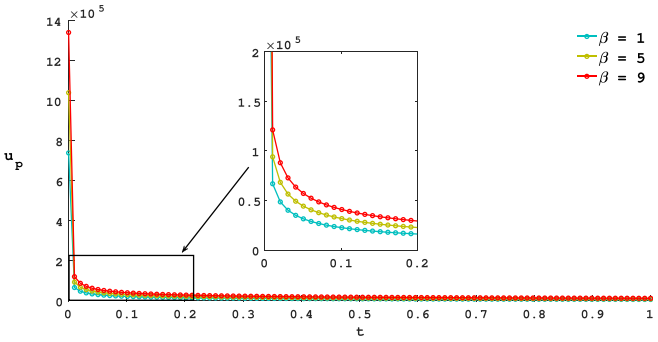

FIG. 10. The variation in the axial velocity of the virus particle with time at fixed values of $\phi = 0.4$, $t = 0.4$, and $x = 0.2$.

addition, we observed that the velocity of the SARS-CoV-2 particle is of the order of 10^5 and, therefore, significantly lower than the spatial velocity distribution shown earlier in Fig. 8. From this result, it is concluded that the virion velocity is non-uniform throughout the blood vessel due to sinusoidal rhythmic contraction and expansion of the moving walls, while at a fixed position, the virion velocity is constant.

Figures 11 and 12 illustrate, respectively, the streamlines of the virion axial velocity and the flow field of the virion for different values of the buoyancy force (Gr) and heat source (β) parameters. From the literature survey, it is observed that the extent of virus enveloping fluid droplets is reduced with diameter due to humidity and temperature impact. Furthermore, the virus can remain in the air for extended periods of time. Mecenas *et al.*[3] considered the case where the droplet size is small due to the removal of liquid contents in the envelope and observed that the virus is expelled at higher temperature, but that this is a slow process. With this in mind, the streamlines of the axial velocity of the virus particle may help to understand the phenomena associated with the SARS-CoV-2 virus flow in a blood vessel. The axial velocity of the virion in the absence of heat generation and thermal buoyancy ($\beta = \mathrm{Gr} = 0$) is observed to decrease as depicted in Fig. 11(a). However, the stream lines of the virion axial velocity are intensified with heat generation and thermal buoyancy, both as shown in Fig. 11(b). The evaporation of liquid contents from the droplets reduces the diameter of enveloped viruses and their density due to high temperature. Therefore, the reduction of virion droplet size and thermal buoyancy force uplifting the droplet increase the velocity magnitude. Corresponding to the virion axial velocity, Fig. 12 represents the movement of the virus particle in the blood vessel. From this result, it is evident that the virion takes time to be activated with greater thermal effects depending on the environment and body temperature. Temperature can reduce the virion influence but will not completely expel the virion. Since the water density is 1000 kg/m^3, which evaporates at 100 °C, however, the SARS-CoV-2 virion density of 1100 kg will modify the overall evaporation temperature of the infected blood. Since the normal human body temperature is around 37.5 °C, this is insufficient to expel the SARS-CoV-2 virus; however, higher temperatures can mitigate to some extent the transmission of virus particles in blood flow.

IV. CONCLUSIONS

A mathematical study of the transient motion of coronavirus particles through blood flow driven by the peristaltic channel has been presented. Thermal buoyancy and heat generation effects are analyzed. The modeling deployed assumes that coronavirus particles with a diameter of 120 μm and a density of 1 g/cm^3 move in the direction of blood flow. The quantity of SARS-CoV-2 virions (entire virus particles) inside a microdroplet is calculated by considering the Kepler conjecture method, and the transmission percentage of viral load is also computed. Computations are performed to visualize the streamline profiles, the variation in the particle relaxation time with particle diameter, the distribution of number of virions (N_p) with SARS-CoV-2 diameter $d_p(\mathrm{nm})$ for different particle diameters, and also the evolution of transmission virions (T_p) with SARS-CoV-2 diameter $d_p(\mathrm{nm})$ for different

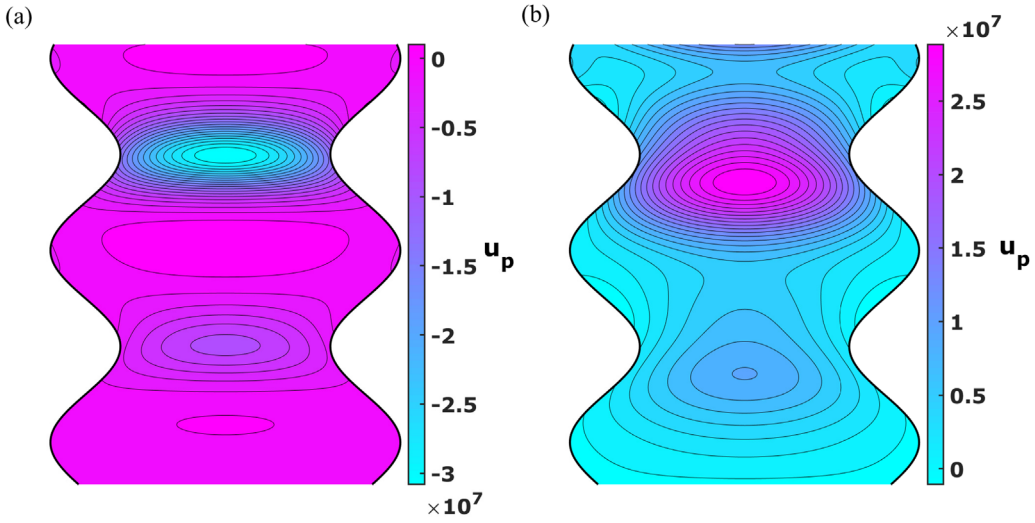

FIG. 11. The streamlines for axial movement of SARS-CoV-2 virus in the blood vessel for (a) no impact of buoyancy force and heat source and (b) the appearance of buoyancy force ($Gr = 2$) and heat source ($\beta = 5$) at fixed values of $\phi = 0.4$, $t = 0.4$, and $x = 0.2$.

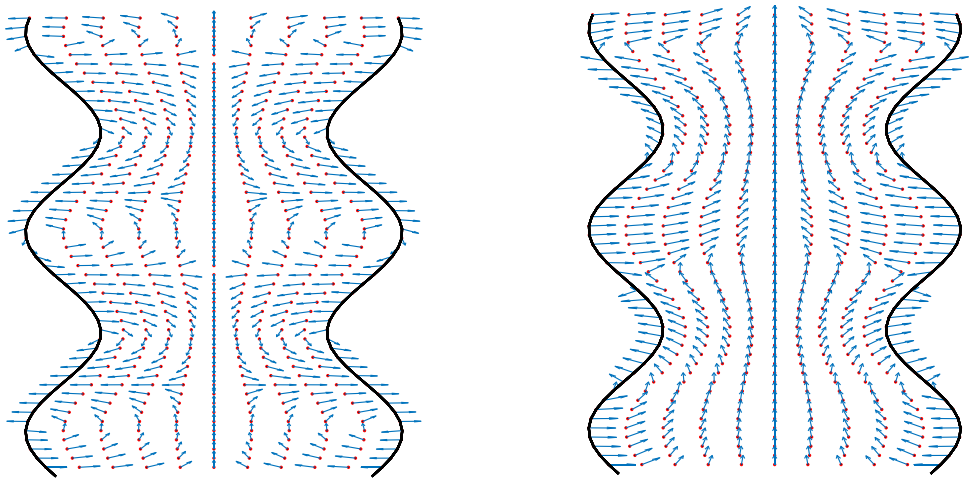

FIG. 12. The flow field of SARS-CoV-2 virus in the blood vessel for (a) no impact of buoyancy force and heat source and (b) the appearance of buoyancy force ($Gr = 2$) and heat source ($\beta = 5$) at fixed values of $\phi = 0.4$, $t = 0.4$, and $x = 0.2$.

virion transmission percentage (V_T). Considering that there is no physical barrier preventing viruses inside the microdroplets, some of the key findings are summarized as follows:

(i) During the interaction, the air route of infection is possible through the infected person to non-infected person via human activity, including coughing, talking, laughing, and sneezing.
(ii) If the percentage of transmission of the SARS-CoV-2 virion is less with a low viral load (the amount of virion that makes a person sick), there are fewer chances to infect another person.
(iii) The small size virus particle ($d_p = 80$ nm) rapidly settles inside the bloodstream as compared to large size virus particles ($d_p = 140$ nm).
(iv) The virus particles can be expelled in humans depending on their anatomy, such as body temperature, lung capacity, surface properties of the lung airways, etc.[31] However, if the SARS-CoV-2 particle remains inside the body for a long time, it can cause damage to blood vessels and tissues.
(v) The evaporation of liquid contents from the droplets reduces the diameter of enveloped viruses and their density due to high temperature.
(vi) Temperature plays a significant role in reducing the package density of the virion droplet, i.e., the cohesion of the particles is reduced with an increment in temperature, so that the SARS-CoV-2 takes greater time to affect the body.

The aim of the present analysis is to provide deeper insights to medical researchers related to how SARS COV-2 viruses behave in peristaltic blood flow with thermal effects, and, furthermore, how body temperature contributes in regulating the transmission of SARS COV-2 and infection in the circulatory system. In the present work, the attention has been confined to the Newtonian fluid model for blood; however, the future investigations may present with non-Newtonian rheological properties of blood.

ACKNOWLEDGMENTS

The authors are grateful to all the reviewers for their excellent comments that have served to improve the paper.

AUTHOR DECLARATIONS

Conflict of Interest

The authors have no conflicts to disclose.

Author Contributions

Dharmendra Tripathi: Conceptualization (equal); Formal analysis (equal); Investigation (equal); Methodology (equal); Supervision (equal); Validation (equal); Writing – review & editing (equal). **D. S. Bhandari:** Formal analysis (equal); Investigation (equal); Methodology (equal); Software (equal); Writing – original draft (equal). **O. Anwar Bég:** Formal analysis (equal); Writing – review & editing (equal).

DATA AVAILABILITY

The data that support the findings of this study are available within the article.

REFERENCES

[1]D. Berry and J. D. Almeida, "The morphological and biological effects of various antisera on avian infectious bronchitis virus," J. Gen. Virol. **3**, 97–102 (1968).
[2]R. Tellier, "Review of aerosol transmission of influenza a virus," Emerging Infect. Dis. **12**, 1657 (2006).
[3]P. Mecenas, R. T. D. R. M. Bastos, A. C. R. Vallinoto, and D. Normando, "Effects of temperature and humidity on the spread of COVID-19: A systematic review," PLoS One **15**, e0238339 (2020).
[4]S. K. Das, J.-E. Alam, S. Plumari, and V. Greco, "Airborne virus transmission under different weather conditions," AIP Adv. **12**, 015019 (2022).
[5]S. E. Haque and M. Rahman, "Association between temperature, humidity, and COVID-19 outbreaks in Bangladesh," Environ. Sci. Policy **114**, 253–255 (2020).

[6]P. C. Woo, S. K. Lau, C.-M. Chu, K.-H. Chan, H.-W. Tsoi, Y. Huang, B. H. Wong, R. W. Poon, J. J. Cai, W.-K. Luk *et al.*, "Characterization and complete genome sequence of a novel coronavirus, coronavirus HKU1, from patients with pneumonia," J. Virol. **79**, 884–895 (2005).
[7]M. R. Maxey and J. J. Riley, "Equation of motion for a small rigid sphere in a nonuniform flow," Phys. Fluids **26**, 883–889 (1983).
[8]M. Bhatti, A. Zeeshan, M. A. Asif, R. Ellahi, and S. M. Sait, "Non-uniform pumping flow model for the couple stress particle-fluid under magnetic effects," Chem. Eng. Commun. **209**, 1058–1012 (2022).
[9]M. M. Bhatti and S. I. Abdelsalam, "Thermodynamic entropy of a magnetized ree-eyring particle-fluid motion with irreversibility process: A mathematical paradigm," ZAMM **101**(6), e202000186 (2021).
[10]M. Bhatti, A. Zeeshan, F. Bashir, S. M. Sait, and R. Ellahi, "Sinusoidal motion of small particles through a Darcy-Brinkman-Forchheimer microchannel filled with non-Newtonian fluid under electro-osmotic forces," J. Taibah Univ. Sci. **15**, 514–529 (2021).
[11]J.-X. Wang, Y.-Y. Li, X.-D. Liu, and X. Cao, "Virus transmission from urinals," Phys. Fluids **32**, 081703 (2020).
[12]M. S. Islam, P. Larpruenrudee, A. R. Paul, G. Paul, T. Gemci, Y. Gu, and S. C. Saha, "SARS CoV-2 aerosol: How far it can travel to the lower airways?," Phys. Fluids **33**, 061903 (2021).
[13]M. S. Islam, P. Larpruenrudee, S. C. Saha, O. Pourmehran, A. R. Paul, T. Gemci, R. Collins, G. Paul, and Y. Gu, "How severe acute respiratory syndrome coronavirus-2 aerosol propagates through the age-specific upper airways," Phys. Fluids **33**, 081911 (2021).
[14]W. H. Finlay, *The Mechanics of Inhaled Pharmaceutical Aerosols: An Introduction* (Academic Press, 2001).
[15]W. Holländer and S. Zaripov, "Hydrodynamically interacting droplets at small Reynolds numbers," Int. J. Multiphase Flow **31**, 53–68 (2005).
[16]S. H. Smith, G. A. Somsen, C. Van Rijn, S. Kooij, L. Van Der Hoek, R. A. Bem, and D. Bonn, "Aerosol persistence in relation to possible transmission of SARS-CoV-2," Phys. Fluids **32**, 107108 (2020).
[17]K. P. Selverov and H. A. Stone, "Peristaltically driven channel flows with applications toward micromixing," Phys. Fluids **13**, 1837–1859 (2001).
[18]N. Ali, S. Hussain, and K. Ullah, "Theoretical analysis of two-layered electro-osmotic peristaltic flow of FENE-P fluid in an axisymmetric tube," Phys. Fluids **32**, 023105 (2020).
[19]N. Ali, K. Ullah, and H. Rasool, "Bifurcation analysis for a two-dimensional peristaltic driven flow of power-law fluid in asymmetric channel," Phys. Fluids **32**, 073104 (2020).
[20]S. Alokaily, K. Feigl, and F. X. Tanner, "Characterization of peristaltic flow during the mixing process in a model human stomach," Phys. Fluids **31**, 103105 (2019).
[21]O. Ashtari, M. Pourjafar-Chelikdani, K. Gharali, and K. Sadeghy, "Peristaltic transport of elliptic particles: A numerical study," Phys. Fluids **34**, 023314 (2022).
[22]A. Bandopadhyay, D. Tripathi, and S. Chakraborty, "Electroosmosis-modulated peristaltic transport in microfluidic channels," Phys. Fluids **28**, 052002 (2016).
[23]J. Chen, K. Gao, R. Wang, D. D. Nguyen, and G.-W. Wei, "Review of COVID-19 antibody therapies," Annu. Rev. Biophys. **50**, 1–30 (2021).
[24]P. R. Vijayaratnam, C. C. O'Brien, J. A. Reizes, T. J. Barber, and E. R. Edelman, "The impact of blood rheology on drug transport in stented arteries: Steady simulations," PLoS One **10**, e0128178 (2015).
[25]T.-Y. Tu and P. C.-P. Chao, "Continuous blood pressure measurement based on a neural network scheme applied with a cuffless sensor," Microsyst. Technol. **24**, 4539–4549 (2018).
[26]H. Minasyan, "Bactericidal capacity of erythrocytes in human cardiovascular system," Int. Clin. Pathol. J. **2**, 00052 (2016).
[27]J. Jiménez-Lozano, M. Sen, and P. F. Dunn, "Particle motion in unsteady two-dimensional peristaltic flow with application to the ureter," Phys. Rev. E **79**, 041901 (2009).
[28]I. Kim, S. Elghobashi, and W. A. Sirignano, "On the equation for spherical-particle motion: Effect of Reynolds and acceleration numbers," J. Fluid Mech. **367**, 221–253 (1998).
[29]A. Issakhov, Y. Zhandaulet, P. Omarova, A. Alimbek, A. Borsikbayeva, and A. Mustafayeva, "A numerical assessment of social distancing of preventing airborne transmission of COVID-19 during different breathing and coughing processes," Sci. Rep. **11**, 9412 (2021).
[30]R. J. Thomas, "Particle size and pathogenicity in the respiratory tract," Virulence **4**, 847–858 (2013).
[31]S. S. Mathews, "A computer simulation study on novel corona virus transmission among the people in a queue," medRxiv (2020).
[32]N. S. M. Nor, C. W. Yip, N. Ibrahim, M. H. Jaafar, Z. Z. Rashid, N. Mustafa, H. H. A. Hamid, K. Chandru, M. T. Latif, P. E. Saw *et al.*, "Particulate matter ($PM_{2.5}$) as a potential SARS-CoV-2 carrier," Sci. Rep. **11**, 2508 (2021).
[33]T. C. Hales, "The sphere packing problem," J. Comput. Appl. Math. **44**, 41–76 (1992).
[34]S. P. Bhat, B. R. Kumar, S. R. Kalamkar, V. Kumar, S. Pathak, and W. Schneider, "Modeling and simulation of the potential indoor airborne transmission of SARS-CoV-2 virus through respiratory droplets," Phys. Fluids **34**(3), 031909 (2022).
[35]J. Gralton, E. Tovey, M.-L. McLaws, and W. D. Rawlinson, "The role of particle size in aerosolised pathogen transmission: A review," J. Infect. **62**, 1–13 (2011).
[36]A. Fernstrom and M. Goldblatt, "Aerobiology and its role in the transmission of infectious diseases," J. Pathog. **2013**, 493960.